2018-04-01

Renal potassium handling in rats with subtotal nephrectomy: modeling and analysis

Renal potassium handling in rats with subtotal nephrectomy: Modeling and Analysis

Running head: K Homeostasis in Subtotal Nephrectomized Kidneys

Anita T. Layton[1], Aurélie Edwards[2], and Volker Vallon[3]

[1]Department of Mathematics, Duke University, Durham, NC 27708-0320, USA;

[2]CNRS ERL 8228, Paris, France, and Department of Biomedical Engineering, Boston University, Boston, MA, USA;

[3]Departments of Medicine and Pharmacology, University of California San Diego, La Jolla, California, and San Diego Veterans Affairs Healthcare System, California.

Direct editorial correspondence to

Anita T. Layton

Department of Mathematics · Duke University · Box 90320 · Durham, NC 27708-0320

Phone: (919) 660-6971 · Facsimile: (919) 660-2821 · E-mail: alayton@math.duke.edu

Abstract

We sought to decipher the mechanisms underlying the kidney's response to changes in K^+ load and intake, under physiological and pathophysiological conditions. To accomplish that goal, we applied a published computational model of epithelial transport along rat nephrons in a sham, uninephrectomized (UNX), and 5/6-nephrectomized (5/6-NX) rats that also considers adaptations in GFR and tubular growth. Model simulations of an acute K^+ load indicate that elevated expression levels and activities of Na^+/K^+-ATPase, epithelial sodium channels (ENaC), large conductance Ca^{2+}-activated K^+ channels (BK), and renal outer medullary K^+ channels (ROMK), together with downregulation of sodium-chloride cotransporters (NCC), increase K^+ secretion along the connecting tubule, resulting in a $>$ 6-fold increase in urinary K^+ excretion in sham rats, which substantially exceeds the filtered K^+ load. In the UNX and 5/6-NX models, the acute K^+ load is predicted to increase K^+ excretion, but at significantly reduced levels compared to sham. Acute K^+ load is accompanied by natriuresis in sham rats. Model simulations suggest that the lesser natriuretic effect observed in the nephrectomized groups may be explained by impaired NCC downregulation in these kidneys. At a single nephron level, a high K^+ intake raises K^+ secretion along the connecting tubule and reabsorption along the collecting duct in sham, and even more in UNX and 5/6-NX. But the increased K^+ secretion per tubule fails to sufficiently compensate for the reduction in nephron number, such that nephrectomized rats have an impaired ability to excrete an acute or chronic K^+ load.

Key words: remnant kidney, epithelial transport, homeostasis, kaliuresis, natriuresis

Introduction

The kidney is the major regulator of potassium (K^+) homeostasis [17]. The primary site for regulation of renal K^+ transport is the distal nephron, which includes the distal convoluted tubule, the connecting tubule, and the cortical collecting duct. It has been established that most of the urinary K^+ excretion can be attributed to tubular secretion [4]. Indeed, urinary K^+ output may exceed the filtered load of K^+ [27]. K^+ secretion into the distal segments is mediated by the renal outer medullary K^+ channel (ROMK), the abundance of which is increased in the distal nephron by aldosterone [46]. Large conductance Ca^{2+}-activated K^+ (BK) channels, expressed in the apical membrane of the distal nephron, may also contribute to K^+ homeostasis, under conditions such as increased tubular flow or a high K^+ diet [28, 33]. K^+ secretion via ROMK and BK channels is driven by a favorable electrochemical gradient established, in part, by Na^+ reabsorption via the epithelial Na^+ channels (ENaC). Thus, K^+ secretion is impacted by Na^+ delivery to the distal segments; that Na^+ delivery is in turn adjusted through changes in sodium-chloride cotransporter (NCC) upstream [39, 42].

When kidney function is sufficiently impaired, plasma $[K^+]$ may rise, resulting in cardiac and neurological disorders. But unlike plasma [urea], the rise of which almost parallels the decline in renal function, plasma $[K^+]$ typically remains within its normal range until the final stage of renal failure [19]. The relative stability of plasma $[K^+]$ indicates an adaptive handling of K^+, such that a progressively larger fraction of filtered K^+ is excreted as glomerular filtration falls. That increased fractional K^+ excretion may be attributed, in part, to the higher distal tubular flow, per nephron, in renal failure [8].

The objective of this study was to examine in a mathematical model the potential mecha-

nisms by which the kidney adapts to increases in K^+ load and intake, under normal conditions or following a loss of functional nephrons.

Modeling Methodology

Model simulations were performed using our published models of epithelial transport along nephrons in the kidney of a sham rat, a uninephrectomized rat (UNX), and a 5/6-nephrectomized rat (5/6-NX) [22]. The models include adaptive changes in GFR and tubular morphology when the nephron number is reduced. The models also represent flow-dependent transport along the proximal tubule, connecting tubule, and cortical collecting duct; in particular, adaptations in Na^+ reabsorption via NCC and flow-dependent Na^+ delivery and ENaC expression level, and thus Na^+ transport-induced K^+ secretion, are included along the distal tubular segments. Model parameters under baseline conditions can be found in Refs. [24, 26, 25, 23, 22].

Simulation of an acute K^+ load. To simulate an acute K^+ load (as KCl) and resulting kidney changes after 2 hours, plasma $[K^+]$ was increased from 4.9 mM to 8.4 mM in sham, to 9.4 mM in UNX, and to 10.4 mM in 5/6-NX, mimicking previous in vivo studies in rats [2, 39] (see Table 1). Note that these plasma $[K^+]$ are higher than those measured 2 hours after an acute K^+ load [1]. This difference is due to our goal to recapitulate urine outputs collected over 2 hours following the K^+ load [1]. Thus, the model required a plasma $[K^+]$ that approximates the average value over that 2-hour period. Plasma $[K^+]$ rises sharply during the first 30 min following a K^+ load, to a value that significantly exceeds that reported after

2 hours in Ref. [1], before gradually decreasing [2, 39]. Thus, the plasma [K^+] chosen to approximate the 2-hour averages are higher than the 2-hour values in Ref. [1]. Plasma [Cl^-] was increased and plasma [Na^+] was decreased such that electroneutrality was maintained and the raise in plasma osmolality was limited to 6 mosm/(kg H_2O). Interstitial fluid [K^+] was also assumed to increase in the inner medulla: at the papillary tip, interstitial [K^+] was increased from 20 mM to 34.4 mM in sham, 38.4 mM in UNX, and 42.4 mM in 5/6-NX. Interstitial [Na^+] was decreased correspondingly. SNGFR was assumed to be unchanged [6]. The expression/activity of NCC along the distal convoluted tubule was decreased by 80% in sham [32]. Additionally, we simulated the effects of K^+-induced aldosterone by increasing the expression/activity of epithelial Na^+ channels (ENaC) by 200% and cortical ROMK by 200%; these changes are consistent with findings reported in Refs. [16, 45]. Expression of BK channels has been reported to increase under high K^+ intake [33]; thus, we assume that under an acute K^+ load, BK channel expression and activity also increase by 200%. Model parameters are shown in Table 1 and discussed further below.

Simulation of a high K^+ diet. To simulate a high K^+ diet, the expression/activity levels of NCC, ENaC, BK, and ROMK were adjusted as observed experimentally [15, 30, 50]; see Table 1. In particular, the expression of apical BK channels was assumed to increase with dietary K^+ intake as previously described [33]. Plasma [K^+] was taken at control levels indicating full compensation [1]. Interstitial fluid [K^+] was taken to be 5 mM above baseline at the outer-inner medullary boundary, and 50 mM above baseline at the papillary tip. Interstitial fluid [Na^+] was reduced correspondingly to leave fluid osmolality unchanged. SNGFR was assumed to be unchanged.

Simulation of an acute K^+ load with high K^+ diet. To simulate the kidney's response to an acute K^+ load under a high K^+ diet, plasma $[K^+]$ was taken to be 0.5 mM less than in the simulations of an acute K^+ load on a control diet, based on [1, 49]; i.e., plasma $[K^+]$ was increased from 4.9 mM to 7.9 mM in sham, to 8.9 mM in UNX, and to 9.9 mM in 5/6-NX [49]. Plasma $[Cl^-]$ and $[Na^+]$ were also adjusted; see Table 1. Changes in transporter expression induced by the K^+ load and by the high K^+ diet cases were assumed to be additive, except for NCC expression level, where we assumed a maximum inhibition of 90%. (Table 1).

Simulation of RAAS blockade. To simulate the effects of aldolsterone inhibition under an acute K^+ load or a high K^+ diet, we reduced the basal and high K^+-induced increases in Na^+/K^+-ATPase, ENaC, ROMK, and BK expression levels [13, 29, 34, 45] (Case 2 values) by 50%. For example, here we assumed that following an acute K^+ load, ENaC expression increased by 100% instead of 200% (compare with Table 1). The adaptations in NCC are assumed not to depend on aldosterone [39].

To simulate the effects of angiotensin converting enzyme (ACE) inhibition under an acute K^+ load or a high K^+ diet, we (i) reduced by 50% the NCC expression level that remains following the K^+ load or diet, (ii) reduced the basal expression levels of Na^+/K^+-ATPase and ROMK by 50%, and (iii) reduced the basal and high K^+-induced increase in ENaC expression levels by 50% [44].

Simulation Results

Simulation of an acute K^+ load. The effects of an acute K^+ load on solute and water transport and urinary excretion in a sham, UNX, and 5/6-NX rat were simulated. Segmental delivery of key solutes and fluid is shown in Fig. 1–4. We first sought to address the question: *To what extent can the higher filtered K^+ load account for the increase in K^+ excretion?* Thus, in the first case ("Case 0"), we incorporated changes in filtered K^+ load but assumed no change in transporter expression levels (see Table 1). The predicted urine flow and excretion rates of Na^+, K^+, Cl^-, and urea are shown in Table 2, under "Acute K^+ load" and labelled "(Case 0)." These values can be interpreted as excretion rates over the first two hours following the acute K^+ load, and can be compared to baseline results, also shown in Table 2. In the second case ("Case 2"), expression/activity levels of NCC, ENaC, BK, and ROMK were also adjusted; see Table 1.

In the sham model, when filtered K^+ load was increased (by 1.7-fold) but tubular transporter protein expression/activity levels were not adjusted (i.e., Case 0), an acute K^+ load increased K^+ excretion by 3.1-fold. When transporter protein expression/activity levels were adjusted (Table 1, Case 2), an acute K^+ load increased K^+ excretion by 6.3-fold. The additional increase in K^+ excretion can be attributed to elevated K^+ secretion along the connecting tubules (a $\sim$6-fold increase). Enhanced distal K^+ secretion was facilitated by a number of factors. First, the downregulation of NCC reduced Na^+ reabsorption along the distal convoluted tubule (see Fig. 5A), thereby increasing Na^+ delivery to the connecting tubule. K^+ secretion along that latter segment is driven in large part by ENaC-mediated Na^+ reabsorption. That exchange was further augmented due to the aldosterone-induced

higher ENaC expression level/activity (see Table 1). Also as a result of NCC downregulation, the higher luminal Na^+ content increased tubular fluid osmolality and reduced water reabsorption in the connecting tubule and cortical collecting duct. The resulting higher tubular flow further elevated transport across ENaC, which is assumed to be flow-dependent [21, 35, 48].

Kaliuresis was accompanied by natriuresis and diuresis. The acute K^+ load raised plasma osmolality by 6 mosm/(kg H_2O) and inhibited the tubular reabsorption of water and Na^+. In particular, the resulting ∼10% decrease in proximal tubule Na^+ reabsorption is shown in Fig. 5A. Consequently, an acute K^+ load raised urine flow by a factor of 2.3 and urinary Na^+ excretion by 69%, compared to baseline conditions (Case 0). The higher urinary K^+ and Na^+ flows were accompanied by elevated urinary Cl^- excretion (∼7-fold of control), to maintain electroneutrality.

The acute K^+ load also increased K^+ excretion in the UNX and 5/6-NX models, albeit to a reduced extent compared to sham. In Case 0 (increased filtered K^+ load only), urinary K^+ excretion was 85 and 60% of sham in the UNX and 5/6-NX models, respectively. In another set of simulations ("Case 1"), we assumed the same changes in transporter expression levels in the nephrectomized models as in sham. Specifically, we assumed a 80% reduction in NCC expression levels in UNX and 5/6-NX. In this case, K^+ excretion was 87 and 59% of sham in the UNX and 5/6-NX models, respectively. Given the reduction in nephron number in the subtotal nephrectomy models, K^+ secretion along the connecting tubule in the UNX and 5/6-NX models would have to be increased to 2 and 6 times, respectively, that of sham in order to attain the same K^+ excretion. That amount of secretion is above the predicted transport capacity of the connecting tubule, despite the elevated ENaC and ROMK expression levels.

As in the sham model, kaliuresis was accompanied by natriuresis. Reabsorption of Na^+ by the proximal tubule and distal convoluted tubule was reduced; see Fig. 5. In both the UNX and 5/6-NX models, the model predicted that urinary Na^+ excretion is similar to that in sham in response to an acute K^+ load (see Table 2).

As noted above, K^+ secretion along the connecting tubule was increased by (i) increased ENaC expression/activity, (ii) reduced NCC expression/activity, and (iii) increased tubular flow. To assess the individual contributions of these factors, we conducted additional simulations using the sham model in which each of these contributing factors was eliminated. Simulation results indicate that ENaC upregulation represents the largest contribution. When ENaC expression was reduced to its baseline level, K^+ secretion along the connecting tubule decreased by ∼40%, resulting in a ∼25% decrease in K^+ excretion. NCC and flow-dependent transport had smaller effects: when changes in each of these factors were eliminated, K^+ secretion and K^+ excretion decreased by <10%.

K^+ load-induced NCC downregulation may be impaired, and Na^+/K^+-ATPase expression/activity may be upregulated, in subtotal nephrectomy models. Contrary to the model's prediction of similar natriuresis (see above), Adam et al. [1] reported that K^+ load-induced natriuresis was attenuated by ∼30% in a nephrectomized rat. Moreover, Sorensen et al. implicated the downregulation of NCC to explain the natriuretic effect of an acute K^+ load in intact kidneys [39].

To eliminate the discrepancy in Na^+ excretion between the model predictions and experimental results, we speculated that NCC downregulation in response to an acute K^+ load may be impaired in a nephrectomized rat [39] and that Na^+/K^+-ATPase expression/activity

may be upregulated along the K^+ secreting segments. To assess the plausibility of that hypothesis, we conducted a second set of simulations (which we refer to as "Case 2"), in which NCC expression was downregulated by 20% (rather than by 80%) by an acute K^+ load in the UNX model, and not at all in the 5/6-NX model. In addition, Na^+/K^+-ATPase expression/activity was increased by 5 and 15%, respectively, along the distal convoluted tubule, connecting tubule, and the collecting duct in UNX and 5/6-NX models. All other assumptions are the same as in Case 0. Model parameters are shown in Table 1. The predicted urine flow and excretion rates of Na^+, K^+, Cl^-, and urea are shown in Table 2, under "Acute K^+ load" and labelled "Case 2". The delivery of selected solutes to individual nephron segments is shown in Figs. 1–4, panels B. These values can be compared to baseline conditions, shown in Table 2 and in Figs. 1–4, panels A. K^+ transport along the distal nephron segments is shown in Fig. 6, top row labelled "Acute K^+ load." Note that results in Fig. 1 are given per animal, whereas those in Fig. 6 are given per nephron.

When downregulation of NCC expression was attenuated and Na^+/K^+-ATPase was upregulated in the UNX and 5/6-NX models, Na^+ delivery to the connecting tubule decreased by $\sim$10% and 5%, relative to its respective value in Case 1. Nonetheless, as shown in Figs. 6A1–6C1, K^+ secretion along an individual connecting tubule was significantly increased in UNX and 5/6-NX compared to sham. However, due to the reduced nephron population, total K^+ secretion along all the connecting tubules was significantly lower in UNX and even more drastically so in 5/6-NX, relative to sham (see Figs. 1B). Consequently, the acute K^+ load raised K^+ excretion in UNX and 5/6-NX to a lesser extent than in sham (82 and 60%, respectively, of sham). The predicted K^+ excretion is only slightly different from Case 0 (85 and 60% of sham, see above). Assuming impaired NCC downregulation and

assuming Na^+/K^+-ATPase upregulation, the model predicted that Na^+ excretion in UNX and 5/6-NX was lowered to 84 and 77% of sham, respectively. These results are consistent with the findings of Adam et al. [1], which indicated that following an acute K^+ load, K^+ and Na^+ excretion in rats with subtotal nephrectomy was lower than that in controls (76 and 41% of control, respectively).

An acute K^+ load substantially increased Na^+/K^+-ATPase-mediated transport along the connecting tubule, to a similar extent among sham, UNX, and 5/6-NX. The increases in Na^+/K^+-ATPase-mediated transport along the distal convoluted tubule and the collecting duct were negligible. Owing to the reduced nephron population in UNX and 5/6-NX, K^+-induced increase in whole-kidney metabolism was much less than in sham. H^+/K^+-ATPase-mediated transport was predicted to be slightly reduced by the acute K^+ load, in all three cases, along the connecting tubule and collecting duct. It is noteworthy that the model predicted enhanced K^+ reabsorption along the collecting duct following an acute K^+ load. Most of that K^+ was reabsorbed via the paracellular pathway, due to the substantially higher luminal $[K^+]$ following a K^+ load. As a result, H^+/K^+-ATPase-mediated transcellular K^+ transport was predicted to decrease slightly.

Effects of varying plasma $[K^+]$. Given that the ability to excrete a K^+ load is impaired in a nephrectomized rat, plasma $[K^+]$ is higher in those animals. Thus, in the above simulations, plasma $[K^+]$ was increased from 4.9 mM to 8.4 mM in sham, to 9.4 mM in UNX, and to 10.4 mM in 5/6-NX [2, 39]. With these assumptions, the model predicted that urinary K^+ excretion is still significantly lower in UNX and 5/6-NX, compared to sham. A question is: *How much must plasma $[K^+]$ be increased in UNX and 5/6-NX for urinary K^+ excretion*

in those models to match that of sham? To answer that question, we conducted simulations of acute K^+ load in which plasma $[K^+]$ was varied over a range of values. Plasma $[Cl^-]$ and $[Na^+]$ were adjusted to maintain electroneutrality and to limit the increase in plasma osmolality to at most 6 mosm/(kg H_2O); see Table 1 for examples.

Predicted urinary K^+ and Na^+ excretion is summarized in Fig. 8. These results were obtained using transport parameters corresponding to Case 2. Results for Cases 0 and 1 are qualitatively similar. Glomerular filtration of K^+ increased proportionally to plasma $[K^+]$. The higher K^+ load raised K^+ excretion, in sham, UNX, as well as 5/6-NX (Fig. 8A). When plasma $[K^+]$ in UNX was increased by 2 mM above its baseline value (from 9.4 to 11.4 mM), urinary K^+ excretion reached baseline sham level. In contrast, at that plasma $[K^+]$ level, the 5/6-NX model generated a urinary K^+ excretion rate that was only 65% of baseline sham level.

Taken in isolation, elevations in K^+ results in net inhibition of water reabsorption, primarily in the proximal tubule. The resulting higher luminal flow lowers the luminal concentration of Na^+, thereby decreasing paracellular Na+ reabsorption in turn. However, increases in plasma $[K^+]$ are accompanied by decreases in plasma $[Na^+]$ (see Table 1) and thus in the filtered load of Na^+. Also, the K^+-induced higher tubular flow upregulates transport across ENaC along the connecting tubule and cortical collecting duct, thereby increasing Na^+ reabsorption along those segments. These competing effects on Na^+ transport are predicted to result in net enhanced Na^+ excretion as plasma $[K^+]$ rises, indicating that the inhibitory effect on water and thus Na^+ in proximal tubules is dominating the response (Fig. 8B).

Effect of variations in interstitial $[K^+]$. Recall that to simulate an acute K^+ load, intersti-

tial fluid [K^+] was assumed to increase in the inner medulla, such that at the papillary tip, interstitial [K^+] was increased from its control value of 20 mM to 34.4 mM in sham, 38.4 mM in UNX, and 42.4 mM in 5/6-NX. We assessed the sensitivity of model results to the elevated interstitial [K^+] (called baseline values). To that end, we conducted simulations in which interstitial [K^+] at the papillary tip was reduced to halfway between the baseline value and the control value (i.e., to 27.2, 29.2, and 31.2 mM in sham, UNX, and 5/6-NX, respectively), and another set of simulations in which papillary tip [K^+] was further reduced to 20 mM. Model results were practically insensitivity to these changes, with urinary K^+ excretion reduced by $< 1.5\%$.

Effects of RAAS blockade. In the next set of simulations, we sought to assess the effects of aldosterone blockade and ACE inhibition on the ability of sham and nephrectomized rats to excrete a K^+ load.

Delivery of selected solutes to individual nephron segments, in the presence of aldosterone inhibition, is shown in Figs. 1–4, panel C. Urinary excretion data are shown in Table 2. With the lower ENaC, ROMK, and BK expression levels mimicking aldosterone inhibition, K^+ secretion along the distal convoluted tubule and connecting tubule in response to an acute K^+ load decreased by 44 and 46%, respectively, in sham, whereas collecting duct K^+ reabsorption, which is mainly paracellular and passive, decreased by 47% (Fig. 6A2). Similar fractional changes in distal K^+ transport were obtained in the UNX and 5/6-NX models. Taken together, the competing effects of aldosterone inhibition on K^+ secretion and Na^+ reabsorption yielded a 44, 44, and 47% reduction in urinary K^+ excretion in sham, UNX, and 5/6-NX, respectively, and 3.6-, 3.5-, and 3.0-fold increases in Na^+ excretion, relative to

the case with full aldosterone effects.

Solute deliveries obtained under ACE inhibition are shown in Figs. 1–4, panel D. Urinary excretion results are shown in Table 2. Like aldosterone blockade, ACE inhibition also led to natriuresis and antikaliuresis, although to a lesser extent: urine K^+ excretion decreased by 13, 14, and 17%, and Na^+ excretion increased by 78, 93, and 80%, respectively, in sham, UNX, and 5/6-NX.

As previously noted, aldosterone blockade and ACE inhibition were simulated by reducing the basal and/or K^+-induced expression levels of transporters that are sensitive to aldosterone or angiotensin II. In the above simulations, the reduction level (which we refer to as "δ") was taken to be 50%. To assess how δ affects model results, we conducted additional simulations in which δ was varied from 0 (no inhibition) to 80% (baseline $\delta = 50\%$ inhibition). The resulting K^+ and Na^+ excretion can be seen in Figs. 7A1 and 7A2 as fractional changes relative to baseline obtained without inhibition. For aldosterone blockade, as δ increased above its baseline value of 50% to 80%, urinary Na^+ excretion approximately doubled and K^+ excretion decreased by 64%. Qualitatively similar changes were obtained for ACE inhibition. For a given inhibition level, aldosterone blockade yielded higher Na^+ excretion and lower K^+ excretion, due to the additional transporter inhibition (Na^+/K^+-ATPase, BK, and ROMK) assumed under aldosterone blockade.

Simulation of a high K^+ diet. In the next set of simulations, we investigated the effects of a high K^+ diet on solute and water transport in the sham, UNX, and 5/6-NX models. These simulations did not include an acute K^+ load and we assumed unchanged plasma K^+ levels. The effects of a high K^+ diet on renal transport were simulated by increasing the

expression levels of ENaC, BK, and ROMK, and downregulating NCC; see Table 1. Again, we first considered the case where changes in transporter expression levels were the same in the sham and nephrectomized models. The predicted urine flow and excretion rates of Na^+, K^+, Cl^-, and urea are shown in Table 3, under "High K^+ diet," labelled "Case 2" for sham and "Case 1" for UNX and 5/6-NX.

The model predicts that, in sham, a high K^+ diet approximately doubles urinary K^+ excretion compared to a control diet, consistent with findings in Ref. [1]. The elevated K^+ excretion can be attributed to the substantial increase in K^+ secretion along the connecting tubule. The mechanisms underlying the increase in K^+ secretion are similar to the acute K^+ load case (see above): augmented ENaC expression/activity, reduced NCC-mediated Na^+ reabsorption, and flow-induced increases in ENaC permeability [9]. A notable difference is that the increase in ENaC expression is smaller with the high K^+ diet compared to an acute K^+ load (40 versus 200%) [16], whereas the downregulation of NCC is attenuated (-50 versus -80%).

Like an acute K^+ load, a high K^+ diet induced natriuresis, albeit to a lesser extent. The downregulation of NCC increased Na^+ delivery to the connecting tubule (by $\sim$60%). On the other hand, the higher ENaC expression level raised Na^+ reabsorption along the connecting tubule; compare insets in Figs. 2A and 2C. These competing factors yielded a $\sim$20% increase in Na^+ flow into the collecting duct and in urinary Na^+ excretion, consistent with findings in Ref. [43]. Owing to the higher K^+ and Na^+ excretion, Cl^- excretion was more than twice of baseline. It is noteworthy that Adam et al. reported that a high K^+ diet induced anti-natriuresis, with a markedly low Na^+ excretion of $\sim$1/3 of baseline [1]. That discrepancy may be attributed to changes in food intake, changes in intestinal transport, an imperfect

salt balance, and/or nuances of K^+ regulation that are not captured by the model (e.g., with no lysine kinases (WNKs) that play a key role in the ability of the kidney to differentially regulate NaCl reabsorption and K^+ excretion).

When changes in transporter expression were assumed to be the same as in sham, and with unchanged plasma [K^+], the UNX and 5/6-NX models predicted increases in Na^+ excretion rates that were similar to those in sham, but K^+ excretion rates were lower, at 87 and 69% of sham for UNX and 5/6-NX, respectively. We then sought to determine what additional adaptations in the transporter set would yield Na^+ and K^+ excretions at approximatly sham levels under a high K^+ diet in UNX and 5/6-NX. *We speculated that some of the aldosterone-induced effects are enhanced in subtotal nephrectomy models on a high K^+ diet.* In particular, we found that further increases in aldosterone-sensitive ENaC, BK, and ROMK expression levels in the nephrectomized kidney models ("Case 2") would achieve this goal. Delivery of selected solutes to individual nephron segments are shown for Case 2 in Figs. 1–4, panels E. With the additional transport parameter changes, the models predicted that, similar to sham, the high K^+ diet elevated K^+ excretion by substantially increasing K^+ secretion into the connecting tubule; see Fig. 1E, and Figs. 6A3 and 6C3.

Effect of variations in interstitial [K^+]. Recall that to simulate a high K^+ diet, interstitial fluid [K^+] was assumed to increase in the inner medulla, such that at the papillary tip, interstitial [K^+] was increased from its control value of 20 mM to its baseline value of 70 mM in sham, UNX, and 5/6-NX. To assess the sensitivity of model results on the elevated interstitial [K^+] we conducted simulations in which interstitial [K^+] at the papillary tip was reduced to halfway between the baseline value and the control value (i.e., 45 mM), and another set

of simulations in which papillary tip [K^+] was further reduced to 20 mM. In sham, these changes resulted in 2 and 8% reduction in urinary K^+ excretion, respectively. Changes in UNX and 5/6-NX were negligible ($< 2\%$ in all cases).

Effects of RAAS blockade. In the next set of simulations, we sought to assess the effects of aldosterone blockade and ACE inhibition on K^+ excretion under a high K^+ diet. Aldosterone inhibition reduced Na^+ reabsorption and K^+ secretion along the connecting tubule and cortical collecting duct. Consequently, urinary K^+ decreased by -44% and Na^+ excretion almost tripled in sham, relative to the case with full aldosterone effects. Results for ACE inhibition, and for UNX and 5/6-NX were qualitatively similar (with generally lesser effects, due to additional transporter inhibition in aldosterone blockade; see above), as shown in Table 3.

Selected transporter parameters were reduced by 50% (δ) to simulate aldosterone blockade and ACE inhibition. To assess the effects of δ on model predictions, we conducted additional simulations in which δ was varied from 0 (no inhibition) to 80% (baseline $\delta = 50\%$). The resulting K^+ and Na^+ excretion can be seen in Figs. 7B1 and 7B2 as fractional changes relative to values obtained without inhibition. For aldosterone blockade, as δ increased above its baseline value of 50% to 80%, urinary Na^+ excretion increased by 5.4-fold and K^+ excretion decreased by 80%. Similar changes were obtained for ACE inhibition.

Simulation of a high K^+ diet and an acute K^+ load. To simulate the kidney's response to an acute K^+ load under a high K^+ diet, transporter parameters were adjusted by combining the changes induced by an acute K^+ load and by a high K^+ diet, as described in Table 1.

Plasma [K^+] was taken to be 0.5 mM lower than in the acute K^+ load cases, consistent with observations in Ref. [1]. Predicted urine flow and excretion rates of Na^+, K^+, Cl^-, and urea are shown in Table 3. Delivery of selected solutes to individual nephron segments is shown in Figs. 1–4, panels F. K^+ transport by distal nephron segments is exhibited in Fig. 6, panels A4–C4.

In the sham model, with a high K^+ diet and an acute K^+ load, K^+ excretion increased by ∼10-fold over basal conditions, and by 23% compared to the case of a control diet with an acute K^+ load. Kaliuresis is accompanied by natriuresis: in this case Na^+ excretion was predicted to be more than double of baseline; see Table 3.

With a high K^+ diet, the acute K^+ load raised K^+ excretion in UNX and 5/6-NX to a lesser extent than in sham. Urinary K^+ excretion rates in UNX and 5/6-NX were predicted to be 85 and 35%, respectively, of sham. These predictions, which are consistent with findings by Adam et al. [1], indicate that the reduced nephron populations in the nephrectomized rat result in similarly impaired K^+ excretion when an acute K^+ load is applied on a normal diet or on top of a high K^+ diet.

Discussion

The kidney has a remarkable ability to maintain the homeostasis of potassium in response to changes in dietary intake. That is accomplished, in part, by modulating the rate of K^+ secretion in distal nephron segments. In patients with renal diseases, serum [K^+] is typically maintained within the normal range without severe restriction of K^+ intake until renal failure progresses to the stage of oliguria [37]. Indeed, with the reduction in functioning renal mass

or nephrons, the diseased kidney, together with enhanced colonic K^+ secretion, is able to maintain K^+ homeostasis by increasing the rate of K^+ excretion by the surviving nephrons [3]. Additionally, the ability to excrete K^+ increases with chronic K^+ loading, although that adaptation is impaired, but not eliminated, in the kidney of a nephrectomized rat [1]. In the current study, we considered the mechanisms underlying the renal response to changes in K^+ load and intake, under physiological and pathophysiological conditions. Key results are summerized in Table 4.

Acute K^+ load induces kaliuresis in a sham rat kidney. Following an acute K^+ load, plasma K^+ and aldosterone levels rise [10, 11]. The elevated filtered K^+ load increases K^+ excretion by >3-fold. An acute K^+ load, through increases in plasma K^+ and aldosterone, also leads to a series of transporter adjustments including enhanced expression of ENaC, BK, and ROMK. Conversely, NCC is downregulated [32]. We assumed a 80% decrease in NCC expression and a doubling in ROMK expression; these values are comparable, respectively, to the measured 60% NCC decrease [32] and 2-fold ROMK increase [38]. Whereas Palmer and Frindt observed a $>$ 10-fold elevation in the density of ENaC in cell-attached patches [31], no change in ENaC protein expression was seen by Rengarajan et al. [32]; the current model assumes a 3-fold increase in response to an acute K^+ load. In the absence of data for BK channels, their expression was taken to increase by 2-fold, same as that of ROMK. With these effects incorporated, the model predicts that in sham, the adaptation in transporter expression increased K^+ secretion along the distal nephron segments, primarily the connecting tubule, and resulted in a $>$ 3-fold increase in urinary K^+ excretion. Combing the elevated filtered K+ and the transporter adaptation increased urinary $K^+ >$ 6-fold. That

predicted increase is lower than the ∼20-fold rise reported by Adam et al. [1], although smaller increases have been observed in other studies (e.g., Ref. [49]).

Reduced nephron number attenuates the kaliuretic effect of an acute K^+ load. This result (Table 2) is consistent with findings by Adam et al. [1], who reported major deficiencies in K^+ excretion in conscious UNX rats following an acute K^+ load. Model predictions are also consistent with another conscious animal study in dogs [5], but in disagreement with anaesthetized rat studies that reported the same or greater levels of K^+ excretion in subtotal nephrectomy groups [3, 36]. The discrepancy remains to be fully elucidated but may be attributed, at least in part, to the effects of anesthetic and the potentially associated effects of sympathetic activation on hemodynamics, or cellular deposition or renal transport of K^+.

The model predicts that following an acute K^+ load, K^+ secretion along an individiual connecting tubule in the kidney of a nephrectomized rat is substantially increased, even more so than in sham, primarily driven by enhanced ENaC-mediated Na^+ reabsorption (Fig. 6). However, due to the reduced nephron population, K^+ excretion in UNX and 5/6-NX falls short of sham (Fig. 1B). The model further predicts that the kidney of a nephrectomized rat reduces overall K^+ reabsorption in the collecting duct system, relative to sham (Fig. 1B). Because K^+ transport along the collecting duct is partly mediated by H^+/K^+-ATPase and thus requires energy, lowering K^+ reabsorption may reduce oxygen consumption and be renal protective. However, the model predicts that elevated K^+ reabsorption in the collecting duct associated with K^+ loading is primarily due to paracellular back-leak and thus does not require enhanced oxygen consumption. It is noteworthy that while the model predicts that

following an acute K^+ load, the UNX rat excretes less K^+ than sham (by 18%), that decrease is less than the ∼50% reduction observed by Adam et al. [1]. The additional difference may be explained by the impaired medullary K^+ cycling in renal failure [18], which yields lower interstitial [K^+] and enhances K^+ reabsorption. Because the present model assumes that interstitial fluid composition is known *a priori*, solute cycling cannot be accurately predicted.

Downregulation of NCC causes natriuresis in sham following an acute K^+ load [39]; NCC downregulation may be impaired in a nephrectomized rat. When NCC was assumed to not be downregulated, the sham model predicted that following an acute K^+ load urinary Na^+ excretion was significantly lower than when NCC was downregulated (by 16%), but it remained significantly higher than without the K^+ load (by 43%). This result implies that there are other factors that contribute to the natriuretic effect of an acute K^+ load on NCC-mediated Na^+ reabsorption. One such factor is that the higher luminal K^+ content increases fluid osmolality and reduces water and thus Na^+ reabsorption. Indeed, when plasma [K^+] was assumed to be 1 mM lower than the baseline (i.e., 7.4 instead of 8.4 mM), the sham model predicted a reduction in Na^+ excretion (by 36%) following an acute K^+ load, accounting for NCC downregulation.

Adam et al. reported a lesser natriuretic effect of an acute KCl load in the renal failure groups [1]. When the same transport changes were assumed in sham and in the nephrectomized kidney models, the model predicted that urinary Na^+ excretion was increased to similar levels following an acute K^+ load in all three groups (Table 2, Case 1). To match the data of Adam et al. [1], we hypothesized that acute NCC downregulation may be impaired and Na^+/K^+-ATPase expression/activity may be upregulated in the kidney of a nephrec-

tomized rat. When these assumptions were applied to UNX and 5/6-NX following an acute K^+ load, the model predicted that Na^+ excretion in UNX and 5/6-NX was 16 and 23% lower than in sham (Table 2, Case 2), consistent with findings by Adam et al. [1].

A sustained high K^+ intake increases urinary K^+ excretion, and enhances the kidney's ability to excrete an acute K^+ load. That has been observed in both control and nephrectomized rats [1, 36]. Many studies have shown that a high K^+ diet modulates the expression of Na^+ and K^+ transporters. In corresponding simulations, we raised the expression of BK by 40% in sham, consistent with observed changes in BK mRNA expression [30]. ENaC abundance was increased by 40% in sham, less than the reported 2-fold increase in γ-ENaC cell-surface expression [15]; but ENaC expression was further increased in the nephrectomized models. NCC expression was halved, similar to the reported 40% decrease [15].

Microperfusion studies suggest that a high K^+ intake or an acute K^+ infusion may also affect water, Na^+, K^+, and Cl^- fluxes in the proximal tubule [7] and the loop of Henle [20, 40, 41]. While there is evidence that a low K^+ diet increases the abundance of NHE3 in rat kidney [12, 14], to our knowledge there are no comparable data on the isolated effects of a high K^+ diet on Na^+ and K^+ transporter expression in the proximal nephron. Apart from flow-mediated effects, transporter abundance in the proximal tubule and thick ascending was therefore kept unchanged in model simulations.

As noted above, model simulations indicate that following an acute K^+ load, K^+ secretion is not attenuated in UNX or 5/6-NX on the single connecting tubule level. The same is true with a high K^+ intake, with or without an acute K^+ load (Fig. 6). But increased K^+ secretion per tubule fails to sufficiently compensate for the reduction in nephron number,

such that nephrectomized rats have an impaired ability to excrete a K^+ load. K^+ excretion is predicted to be insufficient even when plasma [K^+] is assumed to be higher in UNX and 5/6-NX (by 1 and 2 mM, respectively, relative to sham; see Table 1). Model simulations suggest that if plasma [K^+] were increased by an additional 2 mM, urinary K^+ excretion in the UNX model would match sham level. In contrast, as can be seen in Fig. 8, even further increasing plasma [K^+] would not bring K^+ excretion in the 5/6-NX model to sham level.

Effect of RAAS blockade. The model predicts that in sham, with an acute K^+ load, aldosterone blockade results in considerable anti-kaliuresis, whereas ACE inhibition has relatively weaker but still significant effects on K^+ excretion ($\sim$10%, Table 2). Similar fractional decreases are predicted among the sham, UNX, and 5/6-NX model. With high K^+ intake, both aldosterone and ACE blockage yields substantial anti-kaliuresis. The effect of aldosterone blockade is stronger in the nephrectomized models than in sham, and overall weaker with ACE inhibition versus aldosterone blockade (Table 2). A meta-analysis of published clinical studies by Weir and Rolfe [47] concluded that while RAAS inhibitors increase the risk of hyperkalemia in patients with hypertension or cardiovascular renal diseases, those increases are small and similar effects were reported for aldolsterone receptor blockers and ACE inhibitors [47]. Across groups, the present model predicts a smaller effect on urinary K^+ excretion for ACE inhibitors versus aldosterone blockade in particular with an acute K^+ load (see Table 2). That discrepancy may be attributed to the fact that the subjects in Ref. [47] were not K^+-loaded. Another explanation may be the potentially stronger effect of ACE inhibitors in lowering GFR, thereby also compromising K^+ excretion. That latter potential effect was not accounted for by model simulations.

In summary (see also Table 4), our model suggests that following an increase in K^+ intake or acute K^+ load, K^+ secretion increases more significantly in the distal nephron of nephrectomized rats than in control rats, mostly as a result of elevated ENaC-mediated Na^+ reabsorption. However, increased K^+ secretion per nephron is not sufficient to compensate for nephron loss, such that urinary K^+ excretion is lower in nephrectomized rats.

Acknowledgments

This research was supported by the Department of Veterans Affairs (V Vallon) and by the National Institutes of Health: National Institute of Diabetes and Digestive and Kidney Diseases, grants R01DK112042 (V Vallon), R01DK106102 (AT Layton and V Vallon), and the UAB/UCSD O'Brien Center for Acute Kidney Injury Research NIH-P30DK079337 (V Vallon).

References

[1] Adam WR, Adam BA, and Ellis AG. Potassium excretion in renal failure in the rat: The role of distal tubule flow and aldosterone. *Clin Expr Pharmacol Physiol* 15: 619–637, 1988.

[2] Adam WR, Goland GJ, and Wellard RM. Renal potassium adaptation in the rat: role of glucocorticoids and aldosterone. *Am J Physiol (Renal Fluid Electrolyte Physiuol)* 246: F300–F308, 1984.

[3] Bank N and Aynedjian HS. A micropuncture study of potassium excretion by the remnant kidney. *J Clin Invest* 52: 1480–1490, 1973.

[4] Berliner RW. Renal mechanisms for potassium excretion. *Harvey Lact* 55: 141–171, 1961.

[5] Bourgoignie JJ, M Kaplan, J Pincus, G Gavellas, and Rabinovitch A. Renal handling of potassium in dogs with chronic renal insufficiency. *Kidney Int* 20: 482–490, 1981.

[6] Braam B, Boer P, and Koomans HA. Tubuloglomerular feedback and tubular reabsorption during acute potassium loading in rats. *Am J Physiol (Renal Fluid Electrolyte Physiol* 36: F223–F230, 1994.

[7] Brandis M, Keyes J, and Windhager EE. Potassium-induced inhibition of proximal tubular fluid reabsorption in rats. *Am J Physiol* 222: 421–427, 1972.

[8] Buerkert J, Martin D, Prasad J, Chambless S, and Klahr S. Response of deep nephrons and the terminal collecting duct to a reduction in renal mass. *Am J Physiol* 236: F454–F464, 1979.

[9] Carattino MD, Sheng S, and Kleyman TR. Epithelial na^+ channels are activated by laminar shear stress. *J Biol Chem* 279(6): 4120–4126, 2004.

[10] Corvol P, ORLIN ME, Degoulet P, Fressinaud Ph, and Menard J. Effect of acute potassium loading on plasma renin and on urinary aldosterone in rats. *Endocrinology* 100(4): 1008–1013, 1977.

[11] Dluhy RG, Axelrod L, Underwood RH, and Williams GH. Studies of the control of plasma aldosterone concentration in normal man: II. Effect of dietary potassium and acute potassium infusion. *J Clin Invest* 51(8): 1950, 1972.

[12] Elkjær M-L, Kwon T-H, Wang W, Nielsen J, Knepper MA, Frøkiær J, and Nielsen S. Altered expression renal NHE3, TSC, and BSC-1, and ENaC subunits in potassium-depleted rats. *Am J Physiol Renal Physiol* 283: F1376–F1388, 2002.

[13] Estilo G, Liu W, Pastor-Soler N, Mitchell P, Carattino MD, Kleyman TR, and Satlin LM. Effect of aldosterone on BK channel expression in mammalian cortical collecting duct. *Am J Physiol Renal Physiol* 295: F780–F788, 2008.

[14] Frindt G, Houde V, and Palmer LG. Conservation of Na^+ vs. K^+ by the rat cortical collecting duct. *Am J Physiol Renal Physiol* 301: F14–F20, 2011.

[15] Frindt G and Palmer LG. Effects of dietary K on cell-surface expression of renal ion channels and transporters. *Am J Physiol Renal Physiol* 299: F890–F897, 2010.

[16] Frindt G and Palmer LG. Acute effects of aldosterone on the epithelial Na channel in rat kidney. *Am J Physiol Renal Physiol* 308(6): F572–F578, 2015.

[17] Giebisch G, Hebert SC, and Wang WH. New aspects of renal potassium transport. *Pflugers Arch* 446: 289–297, 2003.

[18] Jamison RL. Potassium recycling. *Kidney Int* 31: 695–703, 1987.

[19] Keith NM, King HE, and Osterberg AE. Serum concentration and renal clearance of potassium in severe renal insufficiency in man. *Arch Intern Med* 71: 675–701, 1943.

[20] Kirchner KA. Effect of acute potassium in fusion on loop segment chloride reabsorption in the rat. *Am J Physiol Renal Fluid Electrolyte Physiol* 13: F599–F605, 1983.

[21] Kunau Jr RT, Webb HL, and Borman SC. Characteristics of the relationship between the flow rate of tubular fluid and potassium transport in the distal tubule of the rat. *J Clin Invest* 54(6): 1488, 1974.

[22] Layton AT, Edwards A, and Vallon V. Adaptive changes in GFR, tubular morphology and transport in subtotal nephrectomized kidneys: Modeling and analysis. *Am J Physiol Renal Physiol*, 2017.

[23] Layton AT, Laghmani K, Vallon V, and Edwards A. Solute transport and oxygen consumption along the nephrons: Effects of Na^+ transport inhibitors. *Am J Physiol Renal Physiol* 311: F1217–F1229, 2016.

[24] Layton AT, Vallon V, and Edwards A. Modeling oxygen consumption in the proximal tubule: effects of NHE and SGLT2 inhibition. *Am J Physiol Renal Physiol* 308(12): F1343–F1357, 2015.

[25] Layton AT, Vallon V, and Edwards A. A computational model for simulating solute transport and oxygen consumption along the nephron. *Am J Physiol Renal Physiol* 311: F1378–F1390, 2016.

[26] Layton AT, Vallon V, and Edwards A. Predicted consequences of diabetes and SGLT inhibition on transport and oxygen consumption along a rat nephron. *Am J Physiol Renal Physiol* 310(11): F1269–F1283, 2016.

[27] Leaf A and Camara AA. Renal tubular secretion of potassium in man. *J Clin Invest* 28: 1526–1533, 1949.

[28] Malnic G, Berliner RW, and Giebisch G. Flow dependence of K^+ secretion in cortical distal tubules of the rat. *Am J Physiol* 256: F932–F941, 1989.

[29] Masilamani S, Kim G-H, Mitchell C, Wade JB, and Knepper MA. Aldosterone-mediated regulation of ENaC α, β, and γ subunit proteins in rat kidney. *J Clin Invest* 104(7): R19–R23, 1999.

[30] Najjar F, Zhou H, Morimoto T, Bruns JB, Li H-S, Liu W, Kleyman T R, and Satlin LM. Dietary K^+ regulates apical membrane expression of maxi-K channels in rabbit cortical collecting duct. *Am J Physiol Renal Physiol* 289(4): F922–F932, 2005.

[31] Palmer LG and Frindt G. Regulation of apical K channels in rat cortical collecting tubule during changes in dietary K intake. *Am J Physiol* 277: F805–F812, 1999.

[32] Rengarajan S, Lee DH, Oh YT, Delpire E, Youn JH, and McDonough AA. Increasing plasma [K^+] by intravenous potassium infusion reduces NCC phosphorylation and drives kaliuresis and natriuresis. *Am J Physiol Renal Physiol* 306(9): F1059–F1068, 2014.

[33] Rieg T, Vallon V, Sausbier M, Sausbier U, Kaissling B, Ruth P, and Osswald H. The role of the BK channel in potassium homeostasis and flow-induced renal potassium excretion. *Kidney Int* 72(5): 566–573, 2007.

[34] Salyer SA, Parks J, Barati MT, Lederer ED, Clark BJ, Klein JD, and Khundmiri SJ. Aldosterone regulates Na^+, K^+, ATPase activity in human renal proximal tubule cells through mineralocorticoid receptor. *Biochi Biophy Acta Mole Cell Res* 1833: 2143–2152, 2013.

[35] Satlin LM, Carattino MD, Liu W, and Kleyman TR. Regulation of cation transport in the distal nephron by mechanical forces. *Am J Physiol Renal Phsyiol* 291(5): F923–F931, 2006.

[36] Schon DA, Silva P, and Hayslett JP. Mechanism of potassium excretion in renal insufficiency. *Am J Physiol* 227(6): 1323–1330, 1974.

[37] Seldin DW, Carter NW, and Rector Jr FC. Consequences of renal failure and their management. In: *Diseases of the Kidney* (2ed ed.). Boston: Little Brown and Co, 1971.

[38] Siraskar B, Huang DY, Pakladok T, Siraskar G, Sopjani M, Alesutan I, Kucherenko Y, Almilaji A, Devanathan V, Shumilina E, Föller M, Munoz C, and Lang F. Downregulation of the renal outer medullary K(+) channel ROMK by the AMP-activated protein kinase. *Pfluger Arch* 465: 233–245, 2013.

[39] Sorensen MV, Grossmann S, Roesinger M, Gresko N, Todkar AP, Barmettler G, Ziegler U, Odermatt A, Loffing-Cueni D, and Loffing J. Rapid dephosphorylation of the renal sodium chloride cotransporter in response to oral potassium intake in mice. *Kidney Int* 83: 811–824, 2013.

[40] Stokes JB. Consequences of potassium recycling in the renal medulla. *J Clin Invest* 70: 219–229, 1982.

[41] Unwin R, Capasso G, and Giebisch G. Potassium and sodium transport along the loop of Henle: Effects of altered dietary potassiun intake. *Kidney Int* 46: 1092–1099, 1994.

[42] Vallon V, Schroth J, Lang F, Kuhl D, and Uchida S. Expression and phosphorylation of the Na^+-Cl^- cotransporter NCC in vivo is regulated by dietary salt, potassium, and SGK1. *Am J Physiol Renal Physiol* 297: F704–F712, 2009.

[43] van der Lubbe N, Moes AD, Rosenbaek LL, Shoep S, Meima ME, Danser ALJ, Fenton RA, Zietse R, and Hoorn EJ. K^+-induced natriuresis is preserved during na^+ depletion and accompanied by inhibition of the na^+-cl^- cotransporter. *Am J Physiol Renal Physiol* 305: F1177–F1188, 2013.

[44] van der Lubbe N, Zietse R, and Hoorn EJ. Effects of angiotensin II on kinase-mediated sodium and potassium transport in the distal nephron. *Curr Opin Nephrol Hyperten* 22: 120–126, 2013.

[45] Wald H. Regulation of the ROMK potassium channel in the kidney. *Exp Nephrol* 7: 201–206, 1999.

[46] Wald H, Garty H, Palmer LG, and Popovtzer MM. Differential regulation of ROMK expression in kidney cortex and medulla by aldosterone and potassium. *Am J Physiol* 275: F239–F245, 1998.

[47] Weir WR and Rolfe M. Potassium homeotasis and renin-angiotensin-aldosterone system inhibitors. *Clin J Am Soc Nephrol* 5: 531–548, 2010.

[48] Woda CB, Bragin A, Kleyman TR, and Satlin LM. Flow-dependent K^+ secretion in the cortical collecting duct is mediated by a maxi-K channel. *Am J Physiol Renal Physiol* 280(5): F786–F793, 2001.

[49] Wright FS, Strieder N, Fowler NB, and Giebisch G. Potassium secretion by distal tubule after potassium adaptation. *Am J Physiol* 221: 437–446, 1971.

[50] Yang L, Frindt G, Lang F, Kuhl D, Vallon V, and Palmer LG. SGK1-dependent ENaC processing and trafficking in mice with high dietary K intake and elevated aldosterone. *Am J Physiol Renal Physiol* 312(1): F65–F76, 2017.

Figure 1: Comparison of K^+ delivery obtained for sham, UNX, and 5/6-NX, under baseline conditions (*A*), and the percentage changes, relative to baseline, following an acute K^+ load (*B*), an acute K^+ load with aldosterone (*C*) or ACE (*D*) inhibition, high K^+ diet (*E*), and high K^+ diet and an acute K^+ load (*F*). Results are given per animal. In panel A, colored bars denote superficial nephron values, and are shown above white bars, which denote juxtamedullary nephron values. Height of colored bars denotes whole-kidney values. Panels B–F, changes were obtained for whole-kidney values. PT, proximal tubule; DL, descending limb; mTAL, medullary thick ascending limb; DCT, distal convoluted tubule; CNT, connecting duct; CCD, cortical collecting duct.

Figure 2: Comparison of Na^+ delivery obtained for sham, UNX, and 5/6-NX, under baseline conditions (*A*), an acute K^+ load (*B*), an acute K^+ load with aldosterone (*F*) or ACE (*D*) inhibition, high K^+ diet (*E*), and high K^+ diet and an acute K^+ load (*F*). Results are given per animal. Notations are analogous to those in Fig. 1.

Figure 3: Comparison of Cl^- delivery obtained for sham, UNX, and 5/6-NX, under baseline conditions (*A*), an acute K^+ load (*B*), an acute K^+ load with aldosterone (*C*) or ACE (*D*) inhibition, high K^+ diet (*E*), and high K^+ diet and an acute K^+ load (*F*). Results are given per animal. Notations are analogous to those in Fig. 1.

Figure 4: Comparison of volume delivery obtained for sham, UNX, and 5/6-NX, under baseline conditions (*A*), an acute K^+ load (*B*), an acute K^+ load with aldosterone (*C*) or ACE (*D*) inhibition, high K^+ diet (*E*), and high K^+ diet and an acute K^+ load (*F*). Results are given per animal. Notations are analogous to those in Fig. 1.

Figure 5: Na^+ reabsorption along the proximal tubule, thick ascending limb, and distal convoluted tubule in sham (column *A*), UNX (column *B*), and 5/6-NX (column *C*) rats, given per nephron. White bars, control diet; colored bars, acute K^+ load.

Figure 6: K^+ transport along the distal convoluted tubule, connecting tubule, and collecting duct in sham (column *A*), UNX (column *B*), and 5/6-NX (column *C*) rats, given per nephron. Results were obtained under an acute K^+ load (row 1), acute K^+ load with aldosterone (ALDO) inhibition (row 2), high K^+ diet (row 3), and high K^+ diet with an acute K^+ load (row 4). White bars, control diet; colored bars, acute K^+ load and /or high K^+ diet. K^+ transport is taken positive for reabsorption.

Figure 7: Urinary K^+ excretion (column *1*) and Na^+ excretion (column *2*) in sham following aldosterone or ACE inhibition, simulated by reducing selected transporter parameters to differing degrees. Row *A*, acute K^+ load; row *B*, high K^+ diet. Circles denote baseline inhibition parameter changes, i.e. sham with acute K^+ load or high K^+ diet with $\delta = 50\%$.

Figure 8: Urinary excretion of K^+ (*A*) and Na^+ (*B*) as a function of plasma $[K^+]$, obtained for sham, UNX, and 56-NX under an acute K^+ load. Plasma $[K^+]$ is higher than normal ($\sim$5 mM) to simulate an acute K^+ load. Case 2 parameters were used. Circles denote baseline K^+-induced plasma $[K^+]$ and results. K^+ and Na^+ excretion generally increases as plasma $[K^+]$ increases.

Figure 1:

Figure 2:

Figure 3:

Figure 4:

Figure 5:

Figure 6:

Figure 7:

Figure 8:

Table 1: Transport parameter changes for the sham, UNX, and 5/6-NX models under an acute K^+ load and a high K^+ diet. Under a high K^+ diet alone, plasma $[K^+]$ is taken to be at baseline value. Na^+/K^+-ATPase activity increased along the distal tubule, connecting tubule, and collecting duct only.

	Plasma $[K^+]$	Plasma $[Na^+]$	Plasma $[Cl^-]$	NCC	Na/K-ATPase	ENaC	BK	ROMK
Acute K^+ load								
Sham	8.4 mM	143.5 mM	119.4 mM	−80%	—	+200%	+200%	+200%
UNX (Case 1)	9.4 mM	142.5 mM	119.4 mM	−80%	—	+200%	+200%	+200%
UNX (Case 2)	9.4 mM	142.5 mM	119.4 mM	−20%	+5%	+200%	+200%	+200%
5/6-NX (Case 1)	10.4 mM	141.5 mM	119.4 mM	−80%	—	+200%	+200%	+200%
5/6-NX (Case 2)	10.4 mM	141.5 mM	119.4 mM	—	+15%	+200%	+200%	+200%
High K^+ diet								
Sham	4.9 mM	144.0 mM	116.4 mM	−50%	—	+40%	+20%	+20%
UNX (Case 1)	4.9 mM	144.0 mM	116.4 mM	−50%	—	+40%	+20%	+20%
UNX (Case 2)	4.9 mM	144.0 mM	116.4 mM	−50%	—	+80%	+40%	+40%
5/6-NX (Case 1)	4.9 mM	144.0 mM	116.4 mM	−50%	—	+40%	+20%	+20%
5/6-NX (Case 2)	4.9 mM	144.0 mM	116.4 mM	−50%	—	+200%	+100%	+100%

Table 1 continued

	Plasma [K^+]	Plasma [Na^+]	Plasma [Cl^-]	NCC	Na/K-ATPase	ENaC	BK	ROMK
High K^+ diet + K^+ load								
Sham	7.9 mM	144.0 mM	118.9 mM	−90%	—	+240%	+220%	+220%
UNX (Case 1)	8.9 mM	143.0 mM	119.4 mM	−90%	—	+240%	+220%	+220%
UNX (Case 2)	8.9 mM	143.0 mM	119.4 mM	−70%	+5%	+280%	+240%	+300%
5/6-NX (Case 1)	9.9 mM	142.0 mM	119.4 mM	−90%	—	+240%	+220%	+220%
5/6-NX (Case 2)	9.9 mM	142.0 mM	119.4 mM	−50%	+15%	+400%	+300%	+300%

Table 2: Predicted urinary excretion rates following an acute K^+ load. Values are given per animal.

Urine	Flow (μl/min)	K^+ (μmol/min)	Na^+ (μmol/min)	Cl^- (μmol/min)
	Baseline			
Sham	24	2.6	2.6	2.3
UNX	23	2.6	2.6	3.1
5/6-NX	25	2.7	2.6	4.3
	Acute K^+ load			
Sham (Case 0)	71	8.1	10	15
Sham (Case 2)	78	16	4.6	17
UNX (Case 0)	65	6.9	10	15
UNX (Case 1)	70	13	4.9	16
UNX (Case 2)	63	13	3.8	14
5/6-NX (Case 0)	54	4.9	8.9	13
5/6-NX (Case 1)	57	9.8	5.2	14
5/6-NX (Case 2)	52	9.3	3.5	12
	Acute K^+ load, aldosterone inhibition			
Sham (Case 2)	93	9.0	16	21
UNX (Case 2)	75	7.4	14	18
5/6-NX (Case 2)	59	5.3	10	14
	Acute K^+ load, ACE inhibition			
Sham (Case 2)	83	14	8.1	18
UNX (Case 2)	69	11	7.4	16
5/6-NX (Case 2)	56	8.1	6.3	13

Table 3: Predicted urinary excretion rates with a high K^+ diet. Values are given per animal.

Urine	Flow (μl/min)	K^+ (μmol/min)	Na^+ (μmol/min)	Cl^- (μmol/min)
	High K^+ diet			
Sham (Case 2)	35	5.6	3.2	5.6
UNX (Case 1)	33	4.9	3.6	6.2
UNX (Case 2)	33	5.5	2.9	6.1
5/6-NX (Case 1)	34	3.9	4.4	7.3
5/6-NX (Case 2)	34	5.3	3.0	7.3
	High K^+ diet, aldosterone inhibition			
Sham (Case 2)	49	3.1	10	9.5
UNX (Case 2)	44	2.8	9.0	9.3
5/6-NX (Case 2)	41	2.4	8.0	9.4
	High K^+ diet, ACE inhibition			
Sham (Case 2)	41	3.3	7.1	7.1
UNX (Case 2)	37	3.6	6.1	7.3
5/6-NX (Case 2)	36	4.2	4.7	7.9
	High K^+ diet + acute K^+ load			
Sham (Case 2)	92	20	5.6	22
UNX (Case 2)	77	17	4.8	19
5/6-NX (Case 2)	59	1.2	3.6	14

Table 4: Summary of results

Acute K^+ load in sham:

- elevates filtered K^+ thereby increases urinary K^+ excretion > 3-fold
- induces transporter adaptation (NCC, ENaC, BK, ROMK), which increases urinary K^+ excretion > 3-fold
- total increase in urinary K^+ excretion > 6-fold
- enhances Na^+ excretion due to NCC downregulation and indirect natriuretic effects of enhanced luminal K^+ concentration

High K^+ diet in sham:

- does not change filtered K^+ but induces transporter adaptations (NCC, ENaC, BK, ROMK) that increase urinary K^+ excretion 2-fold; this is also associated with a small natriuretic response
- adaptation to the high K^+ diet enhances/facilitates the kaliuretic and natriuretic response to an additional acute K^+ load

Table 4, continued

Acute K^+ load in UNX/5-6-NX:

- the total increase in urinary K^+ excretion reduces by 18% in UNX and 42% in 5-6-NX versus sham; this occurs despite higher filtration, secretion, and excretion of K^+ on single nephron level; the latter, however, does not fully compensate for reduced nephron number
- the natriuretic response is blunted, possibly due to impaired NCC downregulation and upregulated Na^+/K^+-ATPase expression/activity in the K^+ secreting distal nephron segments

High K^+ diet in UNX/5-6-NX:

- does not change filtered K^+ but induces transporter adaptations (NCC, ENaC, BK, ROMK) similar to sham; this increases urinary K^+ excretion at 87 and 69% of sham for UNX and 5/6-NX, respectively; further increases in aldosterone-sensitive ENaC, BK, and ROMK expression restored urinary K^+ excretion to sham levels; the UNX and 5/6-NX models predict increases in Na^+ excretion rates that are similar to those in sham
- adaptation to the high K^+ diet enhances/facilitates the kaliuretic and natriuretic response to an additional acute K^+ load, but urinary K^+ excretion rates in UNX and 5/6-NX remain 85 and 35%, respectively, of sham, despite higher filtration, secretion, and excretion of K^+ on single nephron level

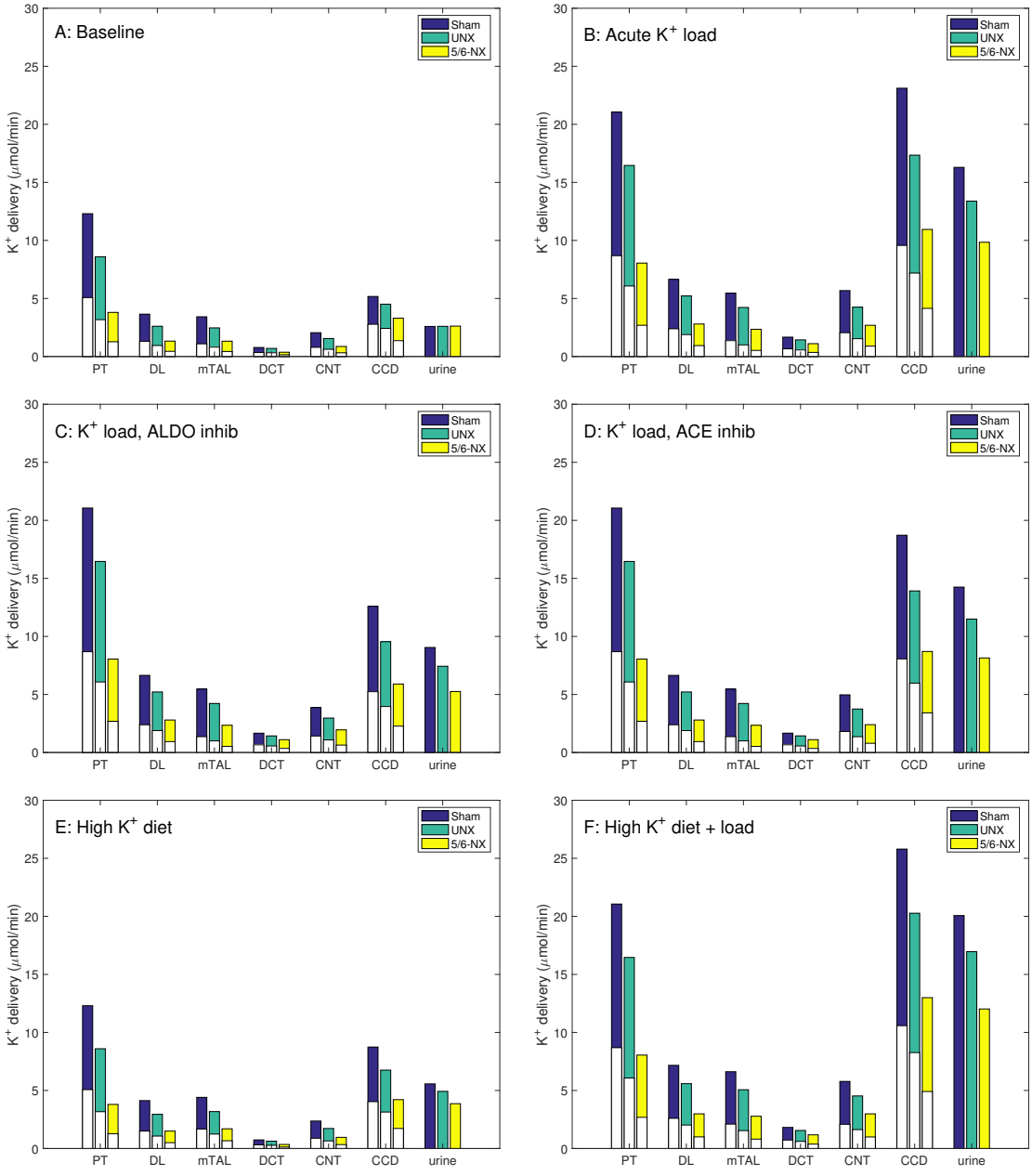
A: Baseline
B: Acute K+ load
C: K+ load, ALDO inhib
D: K+ load, ACE inhib
E: High K+ diet
F: High K+ diet + load
Sham
UNX
5/6-NX
K+ delivery (μmol/min)
PT
DL
mTAL
DCT
CNT
CCD
urine

Figure 1:

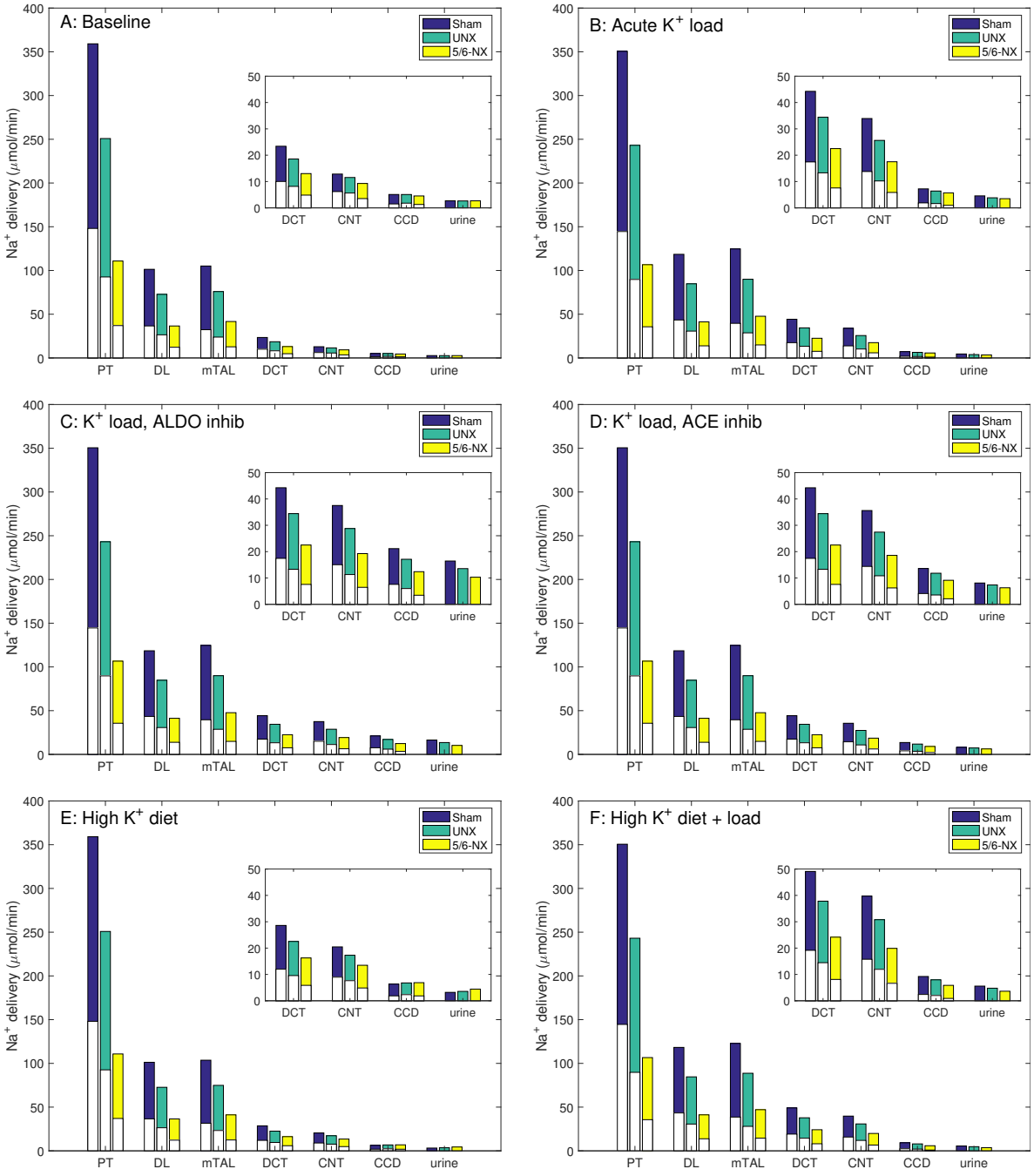
A: Baseline
B: Acute K+ load
C: K+ load, ALDO inhib
D: K+ load, ACE inhib
E: High K+ diet
F: High K+ diet + load
Sham
UNX
5/6-NX
Na+ delivery (μmol/min)
PT
DL
mTAL
DCT
CNT
CCD
urine

Figure 2:

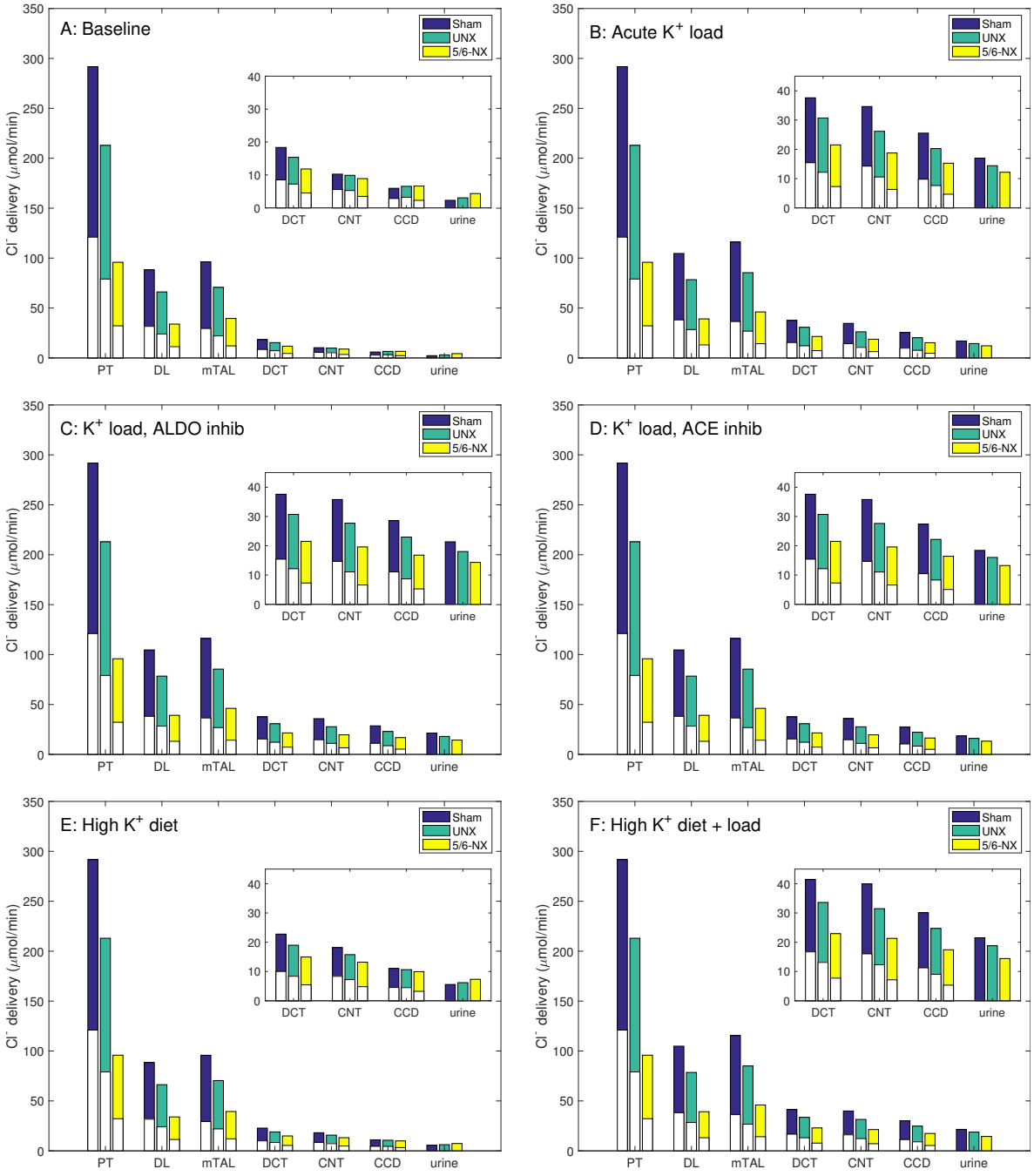
A: Baseline
B: Acute K+ load
C: K+ load, ALDO inhib
D: K+ load, ACE inhib
E: High K+ diet
F: High K+ diet + load
Sham
UNX
5/6-NX
Cl- delivery (μmol/min)
PT
DL
mTAL
DCT
CNT
CCD
urine

Figure 3:

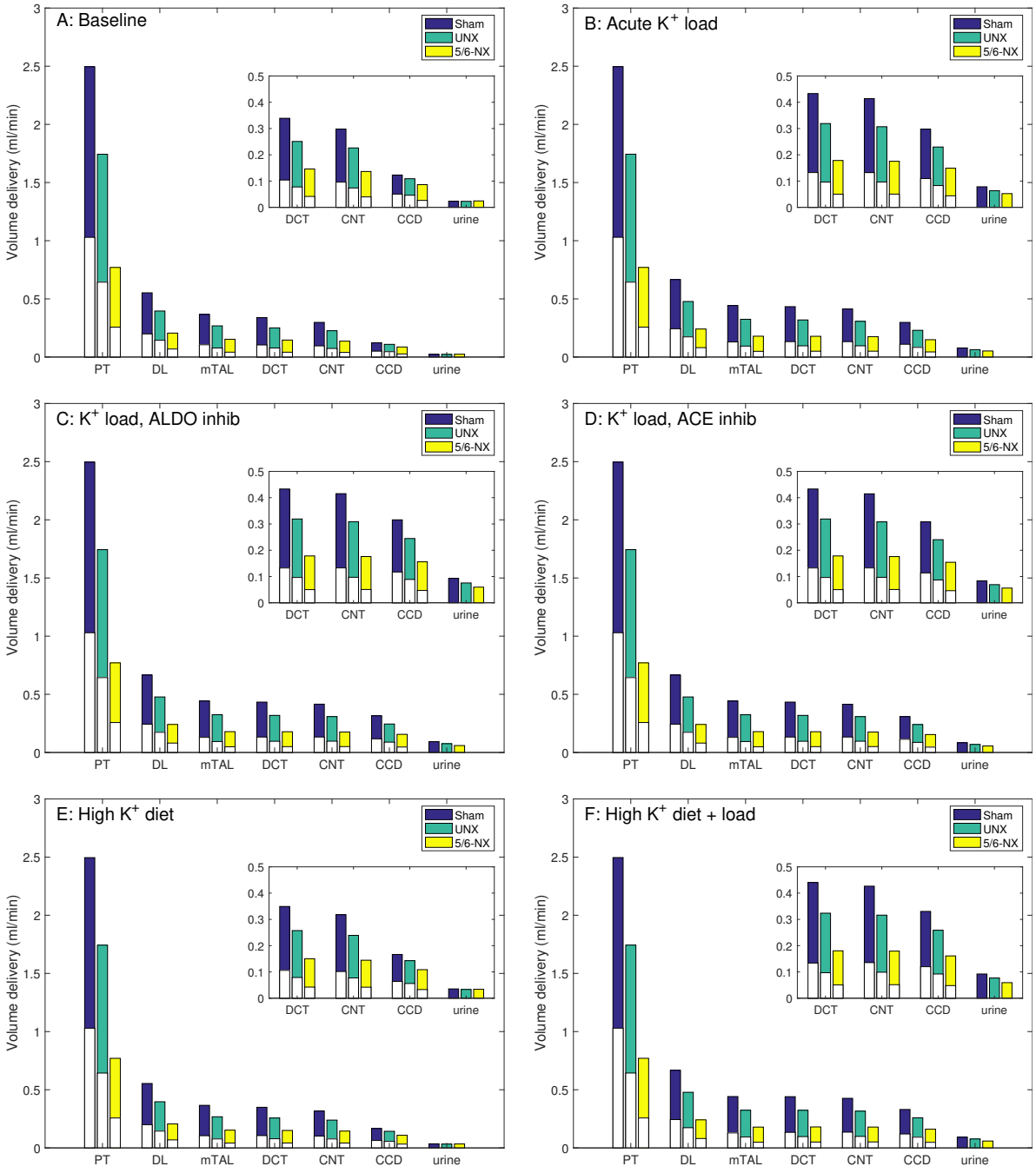
A: Baseline
B: Acute K+ load
C: K+ load, ALDO inhib
D: K+ load, ACE inhib
E: High K+ diet
F: High K+ diet + load
Sham
UNX
5/6-NX
Volume delivery (ml/min)
PT
DL
mTAL
DCT
CNT
CCD
urine

Figure 4:

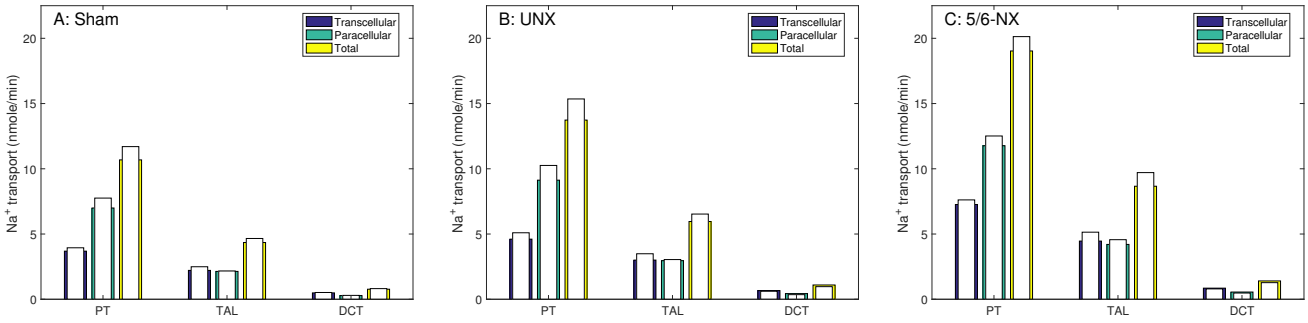
A: Sham
B: UNX
C: 5/6-NX
Transcellular
Paracellular
Total
Na+ transport (nmole/min)
0
5
10
15
20
PT
TAL
DCT

Figure 5:

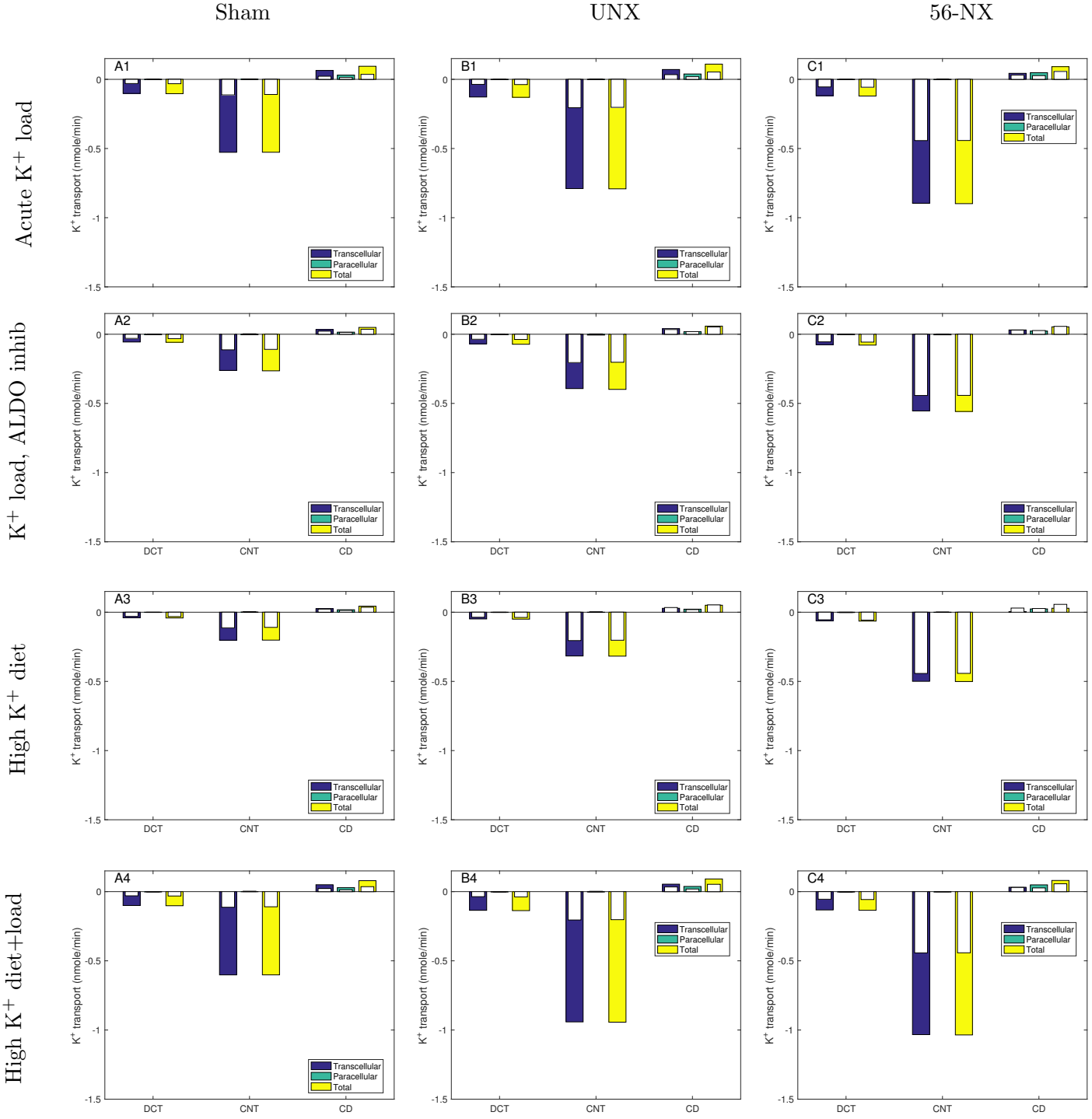
Sham
UNX
56-NX
Acute K+ load
K+ load, ALDO inhib
High K+ diet
High K+ diet+load
A1
B1
C1
A2
B2
C2
A3
B3
C3
A4
B4
C4
K+ transport (nmole/min)
0
-0.5
-1
-1.5
DCT
CNT
CD
Transcellular
Paracellular
Total

Figure 6:

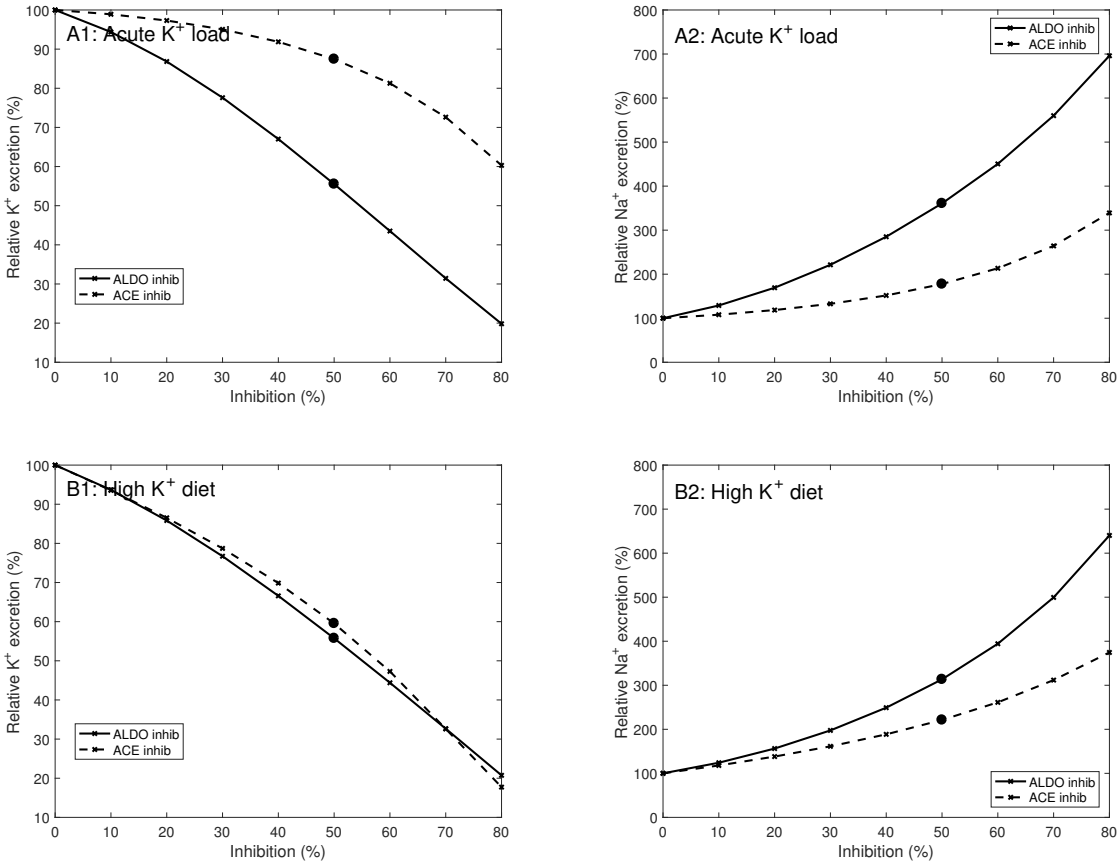
A1: Acute K+ load
A2: Acute K+ load
B1: High K+ diet
B2: High K+ diet
Relative K+ excretion (%)
Relative Na+ excretion (%)
Inhibition (%)
ALDO inhib
ACE inhib

Figure 7:

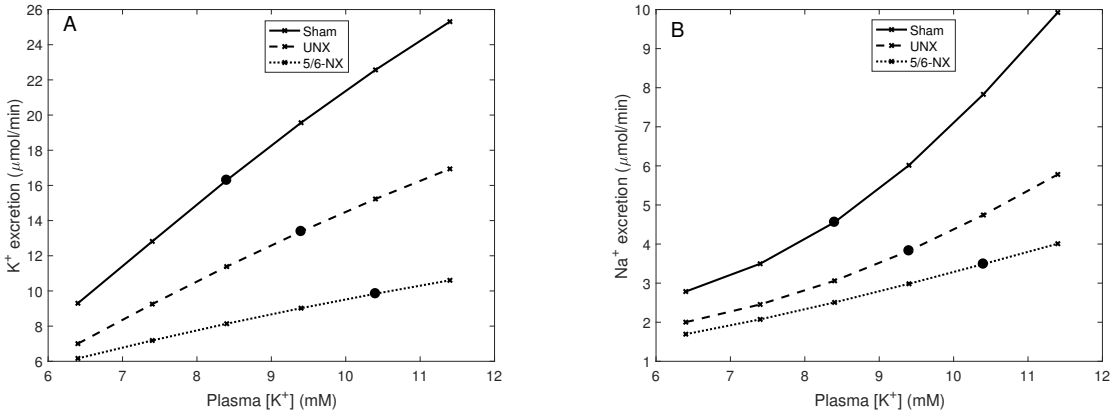
A
Sham
UNX
5/6-NX
K+ excretion (μmol/min)
Plasma [K+] (mM)
B
Sham
UNX
5/6-NX
Na+ excretion (μmol/min)
Plasma [K+] (mM)

Figure 8: